

## **Liquid crystal display surface uniformity defect inspection using analysis of variance and exponentially weighted moving average techniques**

B. C. JIANG<sup>†\*</sup>, C.-C. WANG<sup>‡</sup> and H.-C. LIU<sup>§</sup>

<sup>†</sup>Department of Industrial Engineering and Management, Yuan Ze University,  
Chung-Li, Taiwan 320, ROC

<sup>‡</sup>Graduate School of Engineering Management, Ming Chi University of Technology,  
Taiwan 243, ROC

<sup>§</sup>Chung-Hwa Picture Tubes, Ltd, Taiwan, ROC

*(Received April 2004)*

Display quality is part of the final liquid crystal display (LCD) inspection process before shipping. A 'limited sample' is provided based on the agreement between the manufacturer and the customer. This inspection usually includes an operator who compares the LCD product with the limit sample using the naked eye. The procedure often causes controversy in the manufacturing plant and between the manufacturer and customers. This study attempts to establish a more objective, automatic method to determine the MURA-type defects in LCD panels. A luminance meter is used as the measurement device. An LCD panel is divided into 144 areas. Five points are measured to obtain the luminances. Analysis of variance and the exponentially weighted moving average techniques are applied to determine the existence of MURA defects. Fifty normal LCD panels and 50 MURA defects panels were used to test the inspection method. All 50 LCD panels with MURA defects were correctly identified using the proposed inspection method. The proposed inspection method can help LCD manufacturers reduce the variation in LCD panel inspection results and establish a better relationship with customers through a common inspection mechanism.

**Keywords:** Liquid crystal display (LCD); Defects inspection; Analysis of variance (ANOVA); Exponentially weighted moving average (EWMA)

### **1. Introduction**

The thin-film-transistor-liquid crystal display (TFT-LCD) monitor has recently become the main stream of display devices (Yamazaki *et al.* 1995) because of its smaller space requirement, high-quality display and acceptable cost. Customers demand high-quality product functions and appearance. The LCD panel surface defect inspections are usually performed manually. This process is a labour-intensive, non-value-added part of the production cycle. As higher product quality is required, manufacturers must improve both manufacturing and inspection capabilities.

---

\*Corresponding author. E-mail: iebjiang@saturn.yzu.edu.tw

Most TFT-LCD manufacturers use images generated from simulated signals with operators inspecting the panel with the naked eye. It is easier to inspect defects induced by electronic signals, such as defect lines or points. Non-uniformity defects, normally called MURA defects, are the most difficult to recognize. A 'limit sample' is usually used as the basis for quality judgement. However, controversy often occurs due to the vagueness of the image.

Generally, automatic inspection systems for LCD panel have an optical- or an electrical-based approach. Several electrical or optical-based inspection techniques have been developed for LCD manufacturing. Nevertheless, most existing methods of automatic inspection systems for LCD are based on conventional electrical methods to detect the surface potential. That electrical-based techniques work well for functional verification of an LCD panel. However, they can only be accomplished after the fabrication is completed. In-process inspection may not be applicable to the functional test approach. There is not much research in the literature related to TFT-LCD defect inspection using a vision-based approach. Lu *et al.* (2002) applied a singular value decomposition (SVD) algorithm and developed an image reconstruction scheme for inspecting LCD panel surface defects, such as pinholes, scratches, particles and fingerprints. The SVD algorithm could eliminate the normal texture on the inspected surface, thus concentrating on the defect areas. Lin *et al.* (1998) established a fast image segmentation technique for inspecting the defects on an LCD spacer. Fuzzy set theory was used to determine the threshold for image segmentation. A set of specially designed operation masks was then applied to abstract the features on a spacer. Hwang and Lin (2001) suggested using Houng's transformation technique to calibrate the positional accuracy of an LCD. The defects on the colour filter were thus identified (Wu *et al.* 2000). Kim *et al.* (2001) developed a parallel-operation architecture on a multi-processor vision system for large sized TFT-LCD inspection. A line scan camera was used to obtain a higher resolution image. Four digital signal processors were used to reduce image-processing time. Saitoh (1999) developed a machine vision system for inspecting LCD brightness unevenness. Saitoh first used an edge detection algorithm to detect discontinuous points that included brightness unevenness and noise pixels. A generic algorithm was then applied for detecting the brightness unevenness defects. Previous research did not deal with the LCD panel display non-uniformity problem. The objective of the present study is therefore to establish an automatic inspection process for LCD panel surface uniformity defects.

A major difficulty in TFT-LCD panel non-uniformity inspection is that a good-quality image is difficult to obtain using a regular charge-coupled device (CCD) camera because the camera's grey level resolution is limited. Therefore, a CCD camera used for inspecting a printed circuit board (PCB) (Jiang *et al.* 2001, 2002, Wang and Jiang 2001) would be difficult to use for LCD panel non-uniformity inspection. In this research, a luminance meter, a light-sensitive device, was used to measure panel surface brightness. A data-sampling plan based on the smallest defect area to be detected was designed to collect data effectively for analysis. The analysis of variance (ANOVA) (Montgomery and Runger 2003) and exponentially weighted moving average (EWMA) control chart (Montgomery 2001) concepts were used to detect the non-uniformity areas in a panel. ANOVA was used because the non-uniformity problem between panels is not an issue. The major concern is the non-uniformity (e.g. MURA defects) existing in a given panel; therefore, this

technique could be used to identify areas significantly different from other areas in a panel. The EWMA was applied to detect the small differences in various panel areas.

The TFT-LCD manufacturing process produces numerous product types and defects. The product requirements and defect acceptance levels vary according to customer requirements. This research was conducted under the following conditions:

- Product was limited to 15-inch TFT-LCD modules.
- Manufacturer normally separates these products into higher and lower classes to fulfil various customer needs. Research focused only on the higher class products.
- Manufacturer negotiates with the customer using a 'limit sample', which is used to determine the lower product acceptance level limit. In this research, the limit samples used were samples commonly accepted by general customers.
- According to a common specification, a MURA defect less than  $5 \text{ cm}^2$  can be ignored. This served as the minimum recognized defect size.

## 2. Panel surface defects

There are three types of TFT-LCD display defects: (1) visual appearance defects, (2) electricity induced defects and (3) non-uniform display defects. The first type is caused primarily by the existence of strange articles in the panel, non-uniform colour filter distribution, an uneven space between the upper and lower glass panels, and poor polarizer or back light panel quality. The visual appearance defects mainly include strange particle, spacer clog, white spot, black spot, scratch, operational rubbing fail, rubbing string, strange article, fibre-type article bubble and white spot. The electricity-induced defects are usually caused by poor electrical transmission. These defects appear more regular in shape such as lines or dot defects such as S-line, G-line, SS shot, GS shot, S open, G shift, G open, GS open, luminance defect, black spot defect, continuous spots defect, spot distance, IC poor activation, IC force deviation, poor grey level adjustment, adjustment line defect, feedback circuit defect and power source problem.

Non-uniform display defects appear as an area in which the colour (or grey) is different from the other areas in the panel (figure 1). These defects could appear with a different colour background. These defects might occur due to uneven exposure or other steps in the manufacturing process.

Among the three defect types, the visual appearance defects can be detected using a vision system (Lu *et al.* 2002), the electrically induced defects can be adjusted using conventional electrical methods such an electro-optic modulator (Ryan 1997).









			
GAP Mura	Surrounding GAP	Half-moon GAP	Tr GAP
			
Non-uniform exposure	Non-uniform side angle exposure	Red color GAP	Non-uniform CF color

Figure 1. Common MURA defects in an TFT-LCD.

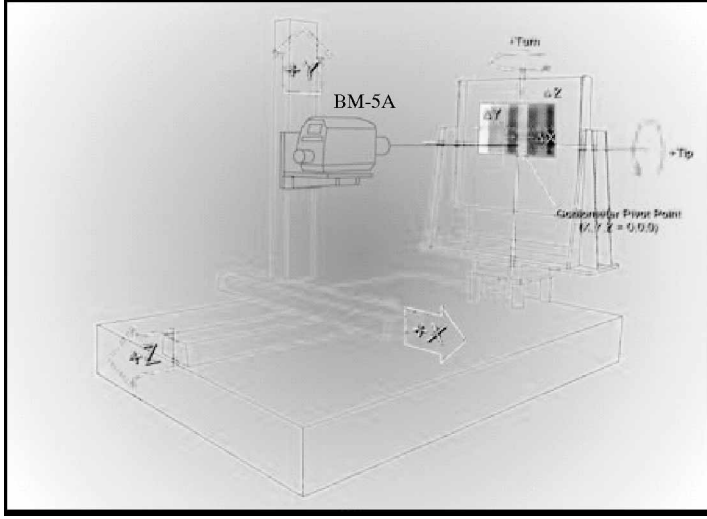


Figure 2. Equipment set-up for data collection.

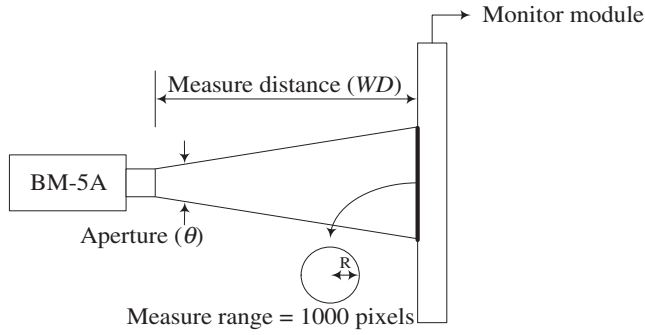


Figure 3. Schematic diagram for data collection.

There is no systematic method for determining the third defect type, the non-uniformity display defect. This research therefore attempts to establish a method for detecting and inspecting non-uniformity display defects.

### 2.1 Panel surface information measurement

A luminance meter (BM-5A) was used to measure the luminance level of a defined area on an TFT-LCD panel. A 1000-pixel area was used for each measurement. Data collection was conducted in a dark room with the panel switched to a white background. The equipment set-up is shown in figure 2. A schematic diagram of the experimental set-up is shown in figure 3.

The relationship between the measurement distance ( $WD$ ), measurement diameter ( $D$ ) and the meter aperture ( $\theta$ ) is:

$$D = 2 \times WD \times \tan(\theta/2). \quad (1)$$

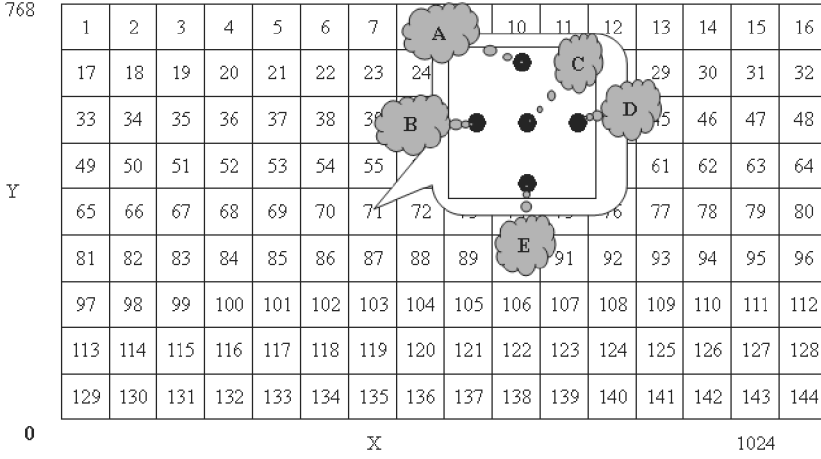


Figure 4. The 144 blocks and five sub-areas on each panel designed for data collection.

Using a 1000-pixel measurement area, the measurement diameter is  $D = 2 \times \sqrt{1000/\pi} \approx 35.6$  pixels. In general, the spacing between two pixels for a 15-inch LCD panel is 0.28 mm. Therefore,  $D \approx 10$  mm. The BM-5A aperture was selected as  $1^\circ$ .  $WD$  can be calculated as follows:

$$WD = \frac{10}{2 \times \tan(0.5^\circ)} \approx 573 \text{ mm}. \quad (2)$$

As noted, a MURA defect less than  $5 \text{ cm}^2$  is usually ignored in the field. A 15-inch TFT-LCD panel was then divided into  $16 \times 9$  blocks at  $4.28 \text{ cm}^2$  each. Five sub-areas with 1000 pixels each were measured in each block. The five sub-areas were the four corners plus centre locations. The data collection design is shown in figure 4. A 15-inch TFT-LCD has  $1024 \times 768 = 786432$  pixels. This is equivalent to 5461 pixels in each of the 144 blocks. The luminance meter measures luminance by collecting an area of 200 pixels of data. Five sub-areas with 5000 pixels of data were collected. This meant that 92% of the pixels were measured in each block. This data collection plan was thought sufficient to detect MURA defects on a TFT-LCD panel.

### 3. Research method

The ANOVA and EWMA techniques were used for data collection and analysis for determining the non-uniform areas and their locations. ANOVA was used to detect if a MURA defect exists on a panel. ANOVA was used because in the LCD non-uniformity problem (such as MURA), there is more concern with non-uniformity on a given LCD panel and there is less concern with the display variation among different panels. Therefore, this technique could be used to identify areas significantly different from other areas in a panel. The EWMA was applied to detect the small differences in various panel areas and to detect position and size of MURA defects.

### 3.1 ANOVA for non-uniformity defect detection

The major purpose for applying ANOVA was to evaluate the difference between the means from several populations (Montgomery and Ruger 2003). One-way ANOVA was used to establish a procedure for evaluating the non-uniformity in a given LCD panel.

Let  $x_{ij}$  be the  $i$ th block and the  $j$ th measurement of a brightness,  $i = 1, 2, \dots, 144$ ;  $j = 1, 2, 3, 4, 5$ . The statistical ANOVA model can be expressed as:

$$x_{ij} = \mu_i + \varepsilon_{ij}. \quad (3)$$

where  $\mu_i$  is the  $i$ th block mean and  $\varepsilon_{ij}$  is the random error term. It is also assumed that the error terms form a normal distribution with mean of 0 and standard deviation of  $\sigma$  (Montgomery and Runger 2003). The following hypothesis test was established according to the defined ANOVA model:

$$\begin{aligned} H_0: \mu_1 &= \mu_2 = \dots = \mu_{144} \\ H_1: &\text{Not all equal.} \end{aligned} \quad (4)$$

If  $H_0$  is rejected, the non-uniformity problem exists on the tested LCD panel. As part of the ANOVA theory, the total sum of squares (SSTO) for the measured values in a block are dissembled into the sum of squares for the treatments (SSTR), the variance within different blocks, and the sum of squares for the random errors (SSE). The mean square treatment (MSTR) and the mean square error (MSE) are obtained by dividing the SSTR and SSE by their degree of freedoms, respectively. If the hypothesis  $H_0$  holds true, both MSTR and MSE represent the unbiased estimates of  $\sigma^2$ . While  $H_0$  is not true, the MSTR will overestimate  $\sigma^2$ , and the MSE is still an unbiased estimate of  $\sigma^2$ . According to this, the MSTR/MSE ratio can be used to judge the degree of difference among the mean measurement block values. It can be statistically proven that the MSTR/MSE is an  $F$  distribution and, therefore, under a decision risk  $\alpha$ , normally set as 0.05, the MSRE/MSE can be compared with the standard  $F$ -value. When  $F_{(143, 576, \alpha)} < (\text{MSTR}/\text{MSE})$ , i.e. accept  $H_0$ , indicating the panel is non-uniform under  $100(1 - \alpha)\%$  confidence.

The set  $\alpha$  level will affect the ANOVA confidence conclusion. Three assumptions are held when conducting ANOVA applications for the validity of a conclusion. The three assumptions are normality, equal variance and independence. The residual analyses with graphical and statistical tests are normally used to verify these three assumptions. Box *et al.* (1987) showed that the  $F$ -test is more robust to the normality assumption if the statistical model is fixed. That is, the ANOVA conclusion is less sensitive to data that violates the normality assumption. The independence nature is critical to the ANOVA application. It is important to collect random data to avoid the data dependency problem.

The procedure for applying ANOVA is summarized as follows:

- Step 1.* Divide an LCD panel into 144 blocks and measure the luminances at five points (i.e. top, bottom, left, right and centre) in each block, denoted as  $x_{ij}$ ,  $i = 1, 2, \dots, 144$ ;  $j = 1, 2, 3, 4, 5$ .
- Step 2.* Calculate the mean and residuals  $e_{ij}$  for each measurement.
- Step 3.* Conduct residual analysis. If the residuals comply with the three assumptions, continue to the next step. Otherwise, make proper data

transformation if the residuals are inappropriate to the normality or equal variance problems exist.

Step 4. Calculate SST and SSE for the collected data:

$$SSTR = \sum_{i=1}^{144} (\bar{x}_i - \bar{\bar{x}})^2, SSE = \sum_{i=1}^{144} \sum_{j=1}^5 (x_{ij} - \bar{x}_i)^2, \quad (5)$$

where

$$\bar{x}_i = \frac{\sum_{j=1}^5 x_{ij}}{5}, \bar{\bar{x}} = \frac{\sum_{i=1}^{144} \sum_{j=1}^5 x_{ij}}{144 \times 5}$$

Step 5. Calculate MSTR and MSE as follows:

$$MSTR = \frac{SSTR}{143}; MSE = \frac{SSE}{576}. \quad (6)$$

Step 6. Calculate  $F = MSTR/MSE$  and then obtain the  $p$ -value for the analysis. If  $p$  is less than the set  $\alpha$ , the LCD panel is determined defective with the MURA problem.

Brightness data were collected from an LCD panel without the MURA defect as previously described, with five points from each of the 144 blocks. Residual analysis was conducted to check the normality, equal variance and independence assumptions. The residual data plots are shown in figure 5. The normality assumption is accepted from the 'normal residual plot' and the 'residual histogram'.

### Residual Analysis

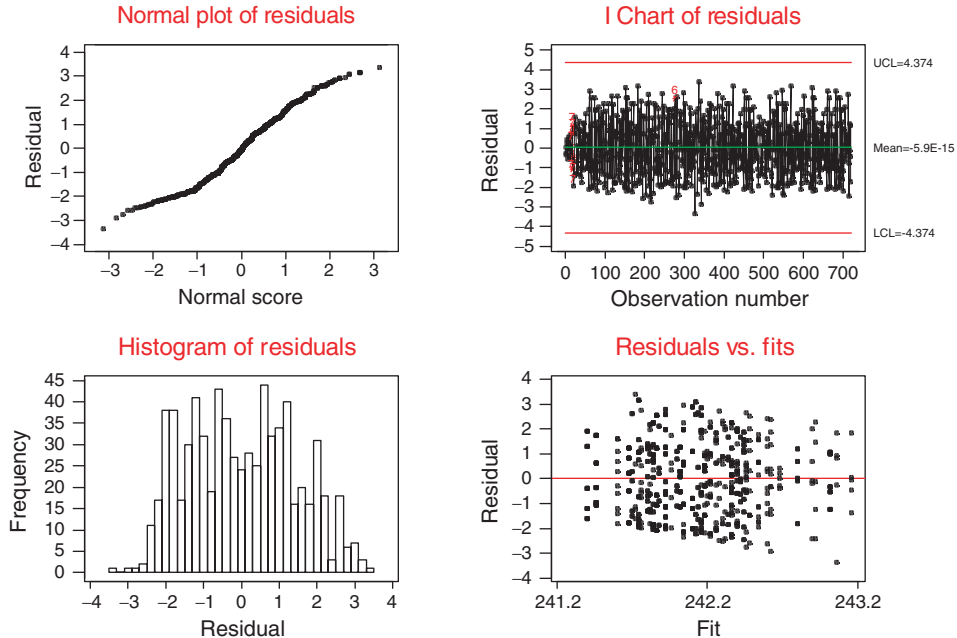


Figure 5. Residual analysis plots for an LCD panel without MURA defects.

Table 1. One-way ANOVA for an LCD panel with MURA defects.

Source	D.F.	Sequential SS	Adjusted SS	Adjusted MS	<i>F</i>	<i>P</i>
Position	143	98.778	98.778	0.691	0.27	1.000
Error	576	1451.660	1451.660	2.520		
Total	719	1550.438				

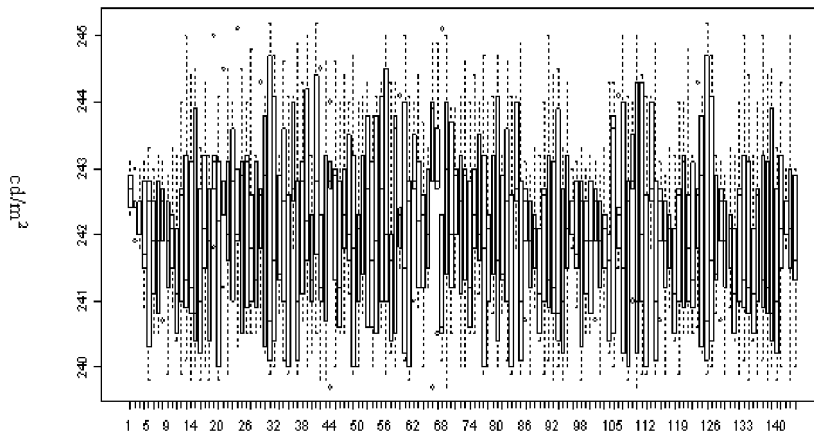


Figure 6. Box plots for the LCD panel with MURA defects.

No particular trend is observed from the ‘Residual I chart’ and ‘Residuals vs. fits’. The equal variance and independence assumptions were also acceptable. A set of statistical tests was conducted to serve as a reference for accepting the three assumptions. The Kolmogorov–Smirnov test, Bartlett and Durbin–Waston tests were used to test normality, equal variance and independence, respectively (Ryan 1997). The results showed that the normality assumption was marginally acceptable and the other two assumptions were confirmed. Because the ANOVA is more robust to the normality assumption, the analysis was continued.

The ANOVA table is shown in table 1. The *p*-value is 1.000. This is much higher than the set  $\alpha$  of 0.05, indicating that the panel has no MURA defects.

The box plots for the tested panel are shown in figure 6. Note that under the 95% confidence level, the 144 data blocks have no significant differences.

An LCD panel with MURA defects was selected for the same procedure. The residual plots are shown in figure 7. From the ‘Residuals vs. fits’ plot, the data are clustered into two bands of areas. A statistical test might be helpful for determining the validity of the equal variance and independence assumptions. Bartlett’s test was used to test the equal variance property (Ryan 1997). The *p*-value was 0.674 and thus the equal variance was accepted. The Durbin–Waston test was used to test the independence assumption. The Durbin–Waston value was 1.92, which is very close to 2, an indication of being independent. Therefore, the ANOVA table was established as shown in table 2. The *p*-value is close to 0, and it is concluded that the panel has significant MURA defects.



## Residual Analysis

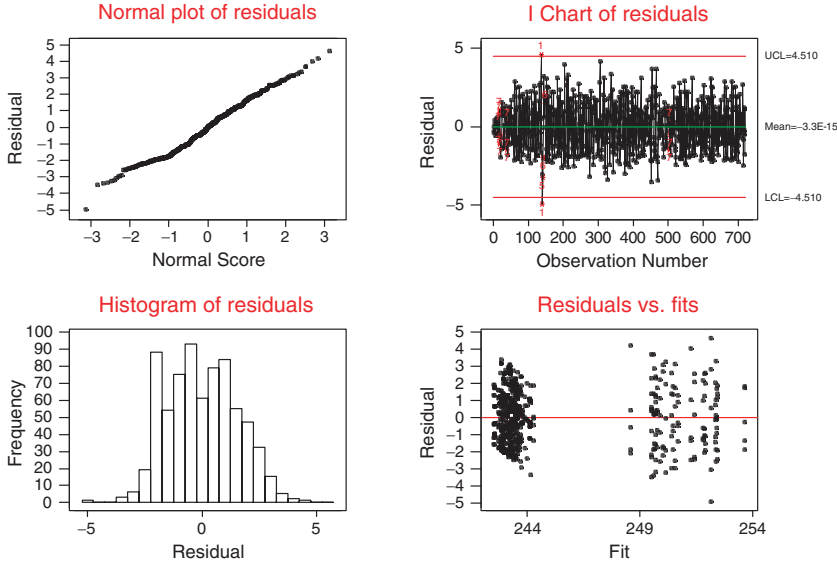


Figure 7. Residual plots for an LCD panel with GAP MURA defects.

Table 2. ANOVA table for an LCD panel with MURA defects.

Source	DF	Sequential SS	Adjusted SS	Adjusted MS	<i>F</i>	<i>P</i>
Position	143	6491.816	6491.816	45.397	15.79	0.000
Error	576	1656.004	1656.004	2.875		
Total	719	8147.820				

The box plots for the tested data are shown in figure 8. Under the 95%, confidence level, at least one block has luminances significantly different from the other blocks.

### 3.2 EWMA for defect position detection

Control charts are normally used for detecting assignable causes of variation (Montgomery 2001). In this study, the control charts concept was used for detecting the position and size of MURA defects, shown as non-uniform luminance on an LCD panel. The measurement data from the 144 blocks were plotted onto the control chart. Because the luminance variation might be slight, the EWMA control chart was selected for this study.

The  $t$ th exponentially weighted moving average  $z_t$  is defined as:

$$z_t = \lambda \bar{x}_t + (1 - \lambda)z_{t-1}, \quad (7)$$

where  $\lambda$  is a smoothing constant, or called weighting constant,  $0 < \lambda \leq 1$ ,  $\bar{x}_t$  is the average of the  $t$ th group data,  $z_t$  is the weighted average for the past data, the initial

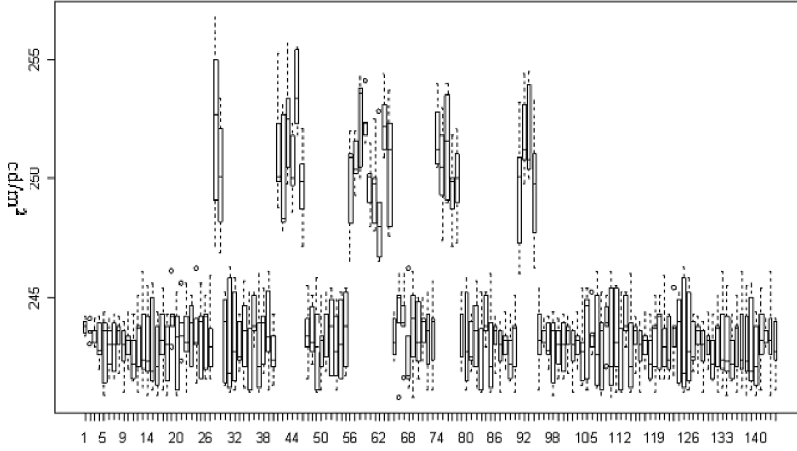


Figure 8. Box plots for an LCD with GAP MURA.

value  $z_0 = \bar{\bar{x}}$ , or an estimate of the mean can be given. The upper and lower limits of the EWMA control chart are as follows (Lucas and Saccucci 1990):

When  $t < 5$ , the upper and lower control limits are:

$$\bar{\bar{x}} \pm 3 \frac{\hat{\sigma}}{\sqrt{n}} \sqrt{\frac{\lambda}{2-\lambda}} [1 - (1-\lambda)^{2t}]; \quad (8)$$

When  $t \geq 5$ ,  $(1-\lambda)^{2t}$  approaches zero, and the upper and lower control limits are

$$\bar{\bar{x}} \pm 3 \frac{\hat{\sigma}}{\sqrt{n}} \sqrt{\frac{\lambda}{2-\lambda}}, \quad (9)$$

where  $\hat{\sigma}$  can be estimated as  $\bar{R}/d_2$  or  $\bar{S}/C_4$ .

The EWMA detection ability is affected by the parameters  $k$  and  $\lambda$ . As a common practice,  $k$  is set as 3.  $\lambda$  is determined using the trial-and-error method. One normal and one defective LCD (with MURA defects) panels were used to determine  $\lambda$ . The MURA position of the defective panel is shown in figure 9. The detection rate for various  $\lambda$  values is shown in figure 10. The detection rate is highest when  $\lambda$  is 0.8. Therefore,  $\lambda$  was set at 0.8 in this study. The resulting EWMA control charts are shown in figure 12.

When  $\lambda = 0.8$ , the blocks were detected as abnormal through the EWMA control chart: 28·29·41·42·43·44·45·46·56·57·58·59·60·61·62·63·64·74·75·76·77·78·91·92·93·94. The MURA area is shown in figure 12. The area is in agreement with the area shown in figure 9.

#### 4. Experiment results

To verify the effectiveness of the developed procedure, 100 LCD panel sample data were collected from a local LCD manufacturer. Among the 100 samples, 50 were normal and the other 50 were defective with six types of MURA defects.



Figure 9. Position of the GAP MURA of an LCD panel.

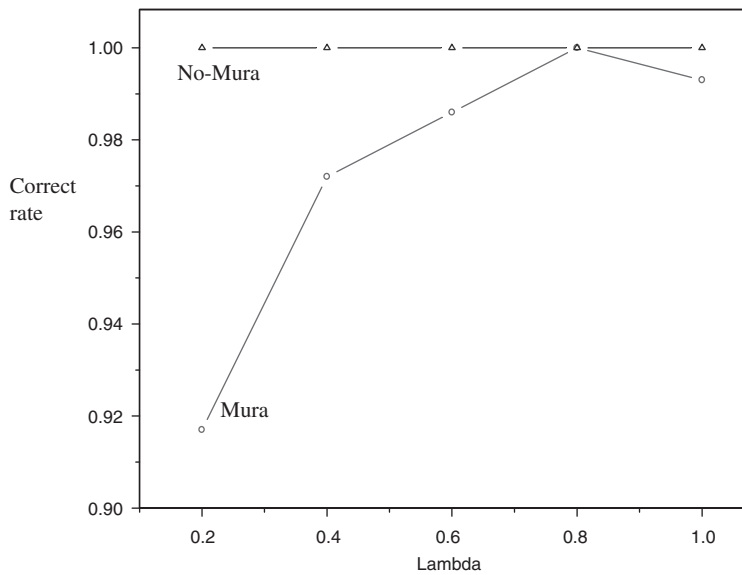


Figure 10. Detection rate for various  $\lambda$  values.

The 50 MURA defect samples include 15 GAP MURA(I), 12 Surrounding GAP(II), 9 Half-moon GAP(III), six Tr GAP(IV), four Non-uniform exposure(V) and four Non-uniform side angle exposure(VI).

The size distribution of the MURA areas in the 50 defective panels is shown in figure 13.

The luminance data were collected using BM-5A equipment. The previously described procedure was followed. The ANOVA was conducted and the  $p$  values were obtained. The EWMA control charts were then used to identify the defective areas. These results were confirmed by an experienced LCD inspection team. The results are shown in table 3. The results showed that all 50 defective LCD panels with six types of MURA defects were identified using the proposed procedure. The defect type, size and location information can then be fed back to manufacturing engineers for process improvement.

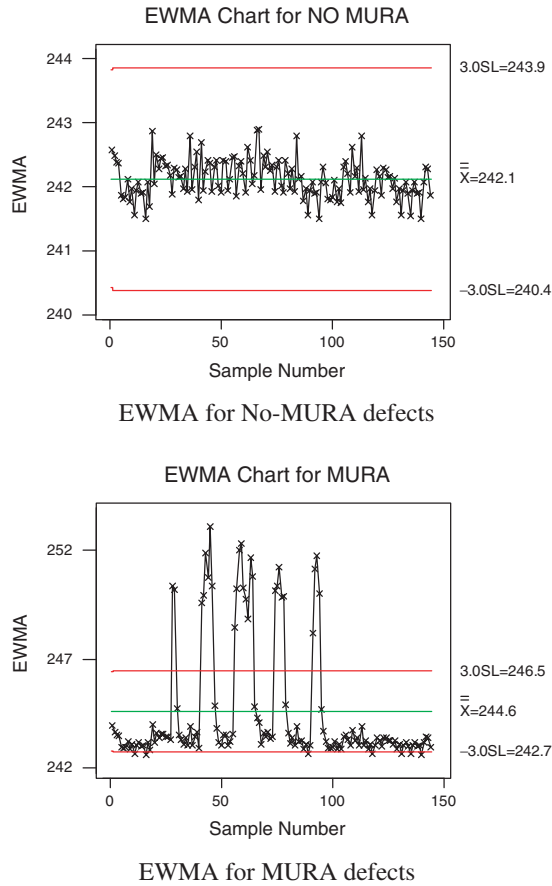


Figure 11. EWMA control charts for normal and MURA LCD panels ( $\lambda=0.8$ ).

1	2	3	4	5	6	7	8	9	10	11	12	13	14	15	16
17	18	19	20	21	22	23	24	25	26	27	28	29	30	31	32
33	34	35	36	37	38	39	40	41	42	43	44	45	46	47	48
49	50	51	52	53	54	55	56	57	58	59	60	61	62	63	64
65	66	67	68	69	70	71	72	73	74	75	76	77	78	79	80
81	82	83	84	85	86	87	88	89	90	91	92	93	94	95	96
97	98	99	100	101	102	103	104	105	106	107	108	109	110	111	112
113	114	115	116	117	118	119	120	121	122	123	124	125	126	127	128
129	130	131	132	133	134	135	136	137	138	139	140	141	142	143	144

Figure 12. MURA area position.

## 5. Conclusion and discussion

An automatic inspection procedure was developed in this study for detecting 15-inch TFT-LCD panel MURA defects. Luminance measurement equipment (BM-5A) was used to collect the needed data for analysis. The first analysis phase involves

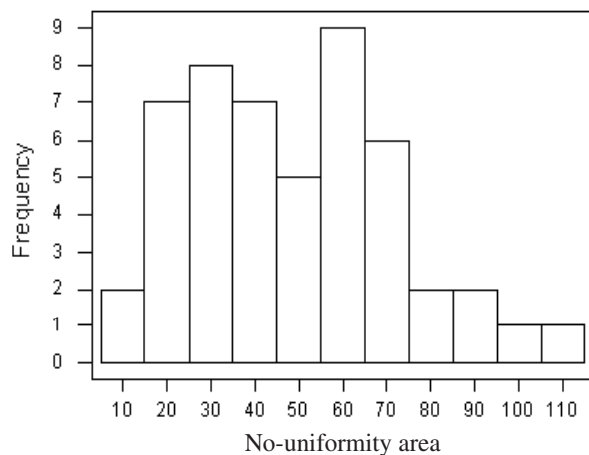


Figure 13. MURA defect area distribution.

		MURA						No-MURA
ANOVA	test sample	50						50
	correct recognized sample	50						50
		I	II	III	IV	V	VI	
EWMA	defect type							
	test sample	15	12	9	6	4	4	
	correct recognized sample	15	12	9	6	4	4	

Figure 14. Flowchart of the proposed LCD MURA defect detection procedure.

with naked eye inspection. (3) The defect type, location and size can be readily obtained. This information can be provided to manufacturing for process improvement. The proposed procedure was limited to 15-inch LCD panels as produced by a local manufacturer. The disadvantage of the proposed procedure is that the  $\lambda$  value is determined through trial and error, and a defective area crossing two of the 144 testing blocks is difficult to identify. The limitations and disadvantages of the results from this study point toward future research areas.

### Acknowledgements

Research was supported by the National Science Council of Taiwan, Project Numbers NSC 91-2213-E-155-034 and NSC 92-2213-E-131-011.

### References

- Box, G.E., Hunter, W.G. and Hunter, J.S., *Statistics for Experimenters*, 1987 (Wiley: New York).
- Hwang, C.S. and Lin, C.S., Study of the application of LCD positioning inspection system, in *The 12th National Automation Technology Conference, 4401B-1, Machine Vision and Image Processing – II*, National Hu-Wei Institute of Technology, 2001.
- Jiang, B.C., Tsai, S.L. and Wang, C.C., Machine-vision based gray relation theory applied to IC marking inspection. *IEEE Trans. Semicond. Manuf.*, 2002, **15**, 531–539.
- Jiang, B.C., Wang, Y.M. and Wang, C.C., Bootstrap sampling technique applied to the PCB golden fingers defect classification study. *Int. J. Prod. Res.*, 2001, **39**, 2215–2230.
- Kim, J.H., Ahn, S., Jeon, J.W. and Byun, J.E., A high-speed high-resolution vision system for the inspection of TFT LCD, in *Proceedings of the ISIE 2001 IEEE International Symposium*, 2001, Vol. 1, pp. 101–105.
- Lin, C.S., Pu, H.C. and Chen, D.C., Using discriminate function and counting mask operation for counting spacers in liquid crystals display plate. *Optik*, 1998, **108**, 133–139.
- Lu, C.J., Tsai, D.M. and Yen, H.N., Automatic defect inspection for LCDs using singular value decomposition, in *Proceedings of the Fourth Asia-Pacific Conference on Industrial Engineering and Management Systems*, Taipei, Taiwan, 2002.
- Lucas, J.M. and Saccucci, M.S., Exponentially weighted moving average control schemes: properties and enhancements. *Technometrics*, 1990, **32**, 1–12.
- Montgomery, D.C., *Introduction to Statistical Quality Control*, 4th edn, 2001 (Wiley: New York).
- Montgomery, D.C. and Runger, G.C., *Applied Statistics and Probability for Engineer*, 3rd edn, 2003 (Wiley: New York).
- Ryan, T.P., *Modern Regression Methods*, 1997 (Wiley: New York).
- Saitoh, F., Boundary extraction of brightness unevenness on LCD display using genetic algorithm based on perceptive grouping factors, in *International Conference on Image Processing*, 1999, vol. 2, pp. 308–312.
- Wang, C.C. and Jiang, B.C., Solder joints defects detection and classification using machine vision. *Int. J. Ind. Eng.*, 2001, **8**, 359–369.
- Wu, M.H., Fuh, C.S. and Chen, H.Y., Defect inspection and analysis of color filter panel. *Image Recogn.*, 2000, **6**, 74–90.
- Yamazaki, T., Kawakami, H. and Hori, H., *Color TFT Liquid Crystal Displays*, 1995 (SEMI Standard FPD Technology Group: Tokyo).